Applied Physics Letters

Femtosecond nonlinear refraction of 2D semi-metallic redox exfoliated $ZrTe_2$ at 800 nm

Cite as: Appl. Phys. Lett. **118**, 011101 (2021); https://doi.org/10.1063/5.0031649
Submitted: 03 October 2020 . Accepted: 18 December 2020 . Published Online: 04 January 2021

Melissa Maldonado, Manoel L. da Silva Neto, Pilar G. Vianna, Henrique B. Ribeiro, Cid B. de Araújo, Christiano J. S. de Matos, Leandro Seixas, Ali M. Jawaid, Robert Busch, Allyson J. Ritter, Richard A. Vaia, and Anderson S. L. Gomes

AIP Publishing

Applied Physics Letters ARTICLE scitation.org/journal/apl

Femtosecond nonlinear refraction of 2D semi-metallic redox exfoliated $ZrTe_2$ at 800 nm

Cite as: Appl. Phys. Lett. **118**, 011101 (2021); doi: 10.1063/5.0031649
Submitted: 3 October 2020 · Accepted: 18 December 2020 ·
Published Online: 4 January 2021

Melissa Maldonado,[1] Manoel L. da Silva Neto,[2] Pilar G. Vianna,[3] Henrique B. Ribeiro,[3] Cid B. de Araújo,[1,2] Christiano J. S. de Matos,[3] Leandro Seixas,[3] Ali M. Jawaid,[4] Robert Busch,[4] Allyson J. Ritter,[4] Richard A. Vaia,[4] and Anderson S. L. Gomes[1,a)]

AFFILIATIONS

[1]Departamento de Física, Universidade Federal de Pernambuco, 50670-901 Recife, PE, Brazil
[2]Graduate Program in Materials Science, Universidade Federal de Pernambuco, 50670-901 Recife, PE, Brazil
[3]MackGraphe, Universidade Presbiteriana Mackenzie, 01302-907 Sao Paulo, SP, Brazil
[4]Materials and Manufacturing Directorate, Air Force Research Laboratories, Wright-Patterson AFB, Ohio 45433, USA

[a)]**Author to whom correspondence should be addressed:** anderson.lgomes@ufpe.br

ABSTRACT

Zirconium telluride, a transition metal dichalcogenide, was synthesized by a redox exfoliated method to obtain a 2D monolayer semi-metal. After being characterized for compositional and optical analysis, its third-order nonlinear optical (NLO) properties were studied by the Z-scan technique in the femtosecond (100 fs) regime at 800 nm. Interestingly, in this spectro-temporal regime and in the intensity range exploited, the only third-order NLO effect observed was nonlinear refraction, giving rise to a positive value of the nonlinear refractive index coefficient, $n_2 = +(4.2 \pm 0.3) \times 10^{-16}$ cm^2/W. Based on the calculated band structure and the excitation photon energies employed, the physical origin of the refractive nonlinearity is discussed.

Published by AIP Publishing. https://doi.org/10.1063/5.0031649

The nonlinear optical (NLO) properties of photonic materials are the basis for several technological applications, from harmonic generation to biomedical imaging.[1] The search for materials with the adequate optical nonlinearities for an expected application has led to the development of a myriad of alternative materials, from bulk organic and inorganic, such as polymers, specialty dyes, and semiconductors, among others,[2] to nanoscale optical materials, including metamaterials[3,4] and nanoscale two-dimensional layered metal dichalcogenides (2D-LTMDs).[5–7] The interest in 2D-LTMDs arose in the last decade after the boom in graphene research,[8] not only to understand their basic properties but also to exploit them in a diversity of applications.[9–11] Most of the literature reports on 2D LTMDs, including NLO basic and applied studies, exploit the semiconducting phase from group VI, MoX_2 (X = S, Se, and Te) and WS_2.[12–14] We have recently reported on NLO properties of the 2D exfoliated metallic NbS_2 monolayer,[15] which belongs to group IVB transition metal dichalcogenides (TMDs).[16]

2D-LTMDs can be synthesized by a variety of methods[8–10] and the modified redox exfoliation (Refs. 17 and 18 and references therein) offers interesting possibilities with technological impact, as in coating and ink technologies, associated with low cost and a general platform for exfoliating LTMDs from group IV, like NbS_2,[15] to group VII, like ReS_2.[16]

In this Letter, we report on the third-order NLO properties of 2D exfoliated semi-metallic zirconium telluride ($ZrTe_2$) monolayers in acetonitrile (ACN) suspension. The samples were prepared by the redox exfoliation method, whose synthesis mechanisms are explained in Ref. 18, and had their compositional analysis carried out by different techniques, including Atomic Force Microscopy (AFM), UV-Vis-near-infrared (NIR) spectroscopy, high resolution transmission electron microscopy (HRTEM), X-ray Photoelectron Spectroscopy (XPS), and Raman Spectroscopy. The NLO studies were carried out using the Z-scan method[19,20] with 800 nm, 100 fs pulses @ 1 kHz. The semi-metallic character of $ZrTe_2$ has been confirmed recently via angle resolved photoemission spectroscopy (ARPES),[21] whereas in Ref. 22, theoretical calculations lead the authors to describe $ZrTe_2$ as being a topological semimetal. Based on our calculation of the band structures of the $ZrTe_2$, which corroborated similarly reported results,[21,23] and the excitation photon energy employed in the experiment, the origin of the nonlinear refraction (NLR) and the absence of nonlinear absorption will be discussed. Samples of the monolayer 2D exfoliated

$ZrTe_2$ TMD used in this work have already been applied as nanoscatterers for random laser action.[24]

The synthesis and morphological characterization of monolayer 2D exfoliated $ZrTe_2$ TMD were described in detail in Refs. 17 and 18. The exfoliation proceeds via *in situ* generation of polyoxometalates (POMs) via redox chemistry. Initially, the bulk powders are suspended in acetonitrile and treated with a mild oxidant (cumyl hydroperoxide), generating soluble metalates in solution. Assembly of these metalates and subsequent adsorption is achieved via addition of reductant (hydroquinone). Adsorption of these polyoxometalates results in delamination via layer charging by assembled POMs.

Extraction of the exfoliated nanomaterial from the bulk nanomaterials is achieved via centrifugal separation. The exfoliated monolayer $ZrTe_2$ flakes are obtained with successive sedimentation and redispersion cycles in fresh anhydrous ACN. Further experimental details, including the stoichiometric chemistries used and reaction durations, can be found in Refs. 17 and 18 and associated supplementary material. Exfoliated monolayer TMD samples were isolated and morphologically and structurally characterized using SEM, AFM, TEM, and XRD.[17,18,24] Nanoflakes with an average thickness of 1.54 ± 0.91 nm and an average lateral extension of 118 ± 53 nm were obtained from AFM and SEM data. Shown in Fig. 1 is the UV-Vis spectra of the $ZrTe_2$ exfoliated samples in ACN (5 μg/ml), recorded on a Cary 5000 Spectrometer[24] with the diffuse reflectance accessory. Initially, absorbance and extinction measurements were obtained from dispersions of the sample, and afterwards, scattering profiles were obtained by subtracting the extinction spectra from absorbance spectra, where $\mathrm{Ext}(\lambda) = \mathrm{Abs}(\lambda) + \mathrm{Sca}(\lambda)$, as shown in Fig. 1. Careful analysis and extrapolation of the absorption curve indicate an absorption onset at ~0 eV, which is in line with the semi-metallic character of the material.

The NLO characterization used the well-established Z-scan method,[19] recently reviewed in Ref. 20. In short, it relies on the induced wave front distortion due to the spatial self-phase modulation arising from the nonlinear refractive index of the medium. The sample

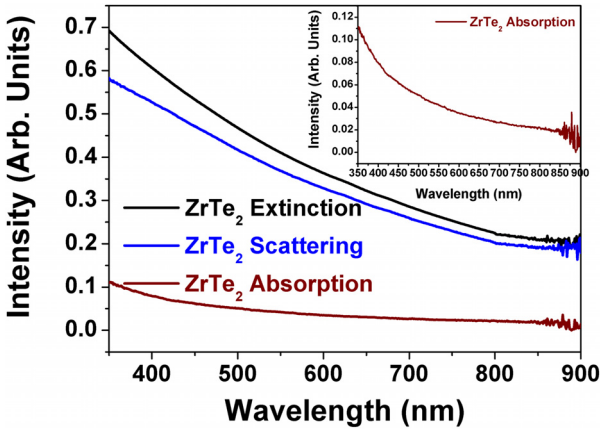

FIG. 1. UV-Vis spectroscopy was performed on $ZrTe_2$ dispersions in acetonitrile (5 μg/ml). The extinction and absorbance values were measured, and extraction of the scattering profile was obtained via $\mathrm{Extinction}(\lambda) - \mathrm{Absorption}(\lambda) = \mathrm{Scatter}(\lambda)$. Note that, due to the metallic nature of $ZrTe_2$, the absorption curves are featureless. The noise in the 850 nm–900 nm region is due to the end of the spectrometer range.

is scanned in the Z-direction of a focused beam, and the transmitted light is collected by a photodetector (PD). If a small aperture is placed in front of the PD, the nonlinear refraction (NLR) is directly measured in sign and magnitude, given that the beam intensity is known. If the whole beam is collected, the nonlinear absorption (NLA) is obtained, which can have several origins.[20] The equations to obtain the NLR and NLA coefficients are well known as derived and described in Refs. 19 and 20. In the experimental setup employed, simultaneous measurements of the NLR and NLA were obtained, which were also normalized to the shot-to-shot fluctuations of the excitation source. The light source was a Ti:sapphire-based regenerative amplifier (800 nm) operating at 1 kHz and delivering 100 fs single pulses with the maximum energy of 1 mJ. The beam was focused with a 15 cm focal length lens onto a 1 mm quartz cuvette. The peak intensity was varied up to $I = 140\ \mathrm{GW/cm^2}$ (corresponding to a maximum fluence $F = 75.6\ \mathrm{mJ/cm^2}$) for the present experiment. The nonlinear (NL) refractive index (n_{NL}) and NLA coefficient (α_{NL}) were measured, from which the values of Re $\chi^{(3)}$ and Im $\chi^{(3)}$ could be inferred.

As a control experiment, Z-scan measurements were initially performed for the solvent, pure ACN, which showed a positive (self-focusing) NLR with the value of $n_2 = 1.9 \times 10^{-17}\ \mathrm{cm^2/W}$, compatible with the literature,[25] as shown in Figs. 2(a) and 2(b). The $n_2 \times I$ curve shown in Fig. 2(b) was a constant, indicating that third-order NLR was the dominant mechanism at such excitation conditions. Open aperture measurements did not show any results for the range of intensities employed and, therefore, NLA was negligible. Figures 2(c) and 2(d) show the NLR result for $ZrTe_2$, which behaved qualitatively similar to the solvent, with the same positive sign for the NLR.

Similar to the solvent, NLA was not observed in the range of intensities employed for the 2D exfoliated $ZrTe_2$ suspension. NLA can arise, for instance, from one- or two-photon absorption, saturated absorption, or reverse saturated absorption, among others. All these phenomena have been identified in MoS_2 and WS_2[12–14] at intensities higher than $200\ \mathrm{GW/cm^2}$ and using appropriate excitation photon energies compared to the bandgap of the material studied, including the equivalent wavelength of 800 nm. Furthermore, in the recent work on 2D exfoliated NbS_2 suspended in ACN and prepared by the same method as in this work, NLR and NLA were measured in the same experimental conditions as in the present work. It is important to remind the metallic nature of the exfoliated NbS_2 suspension.

To determine the NLR coefficient, we employed the known equation for the closed aperture Z-scan:[19,20]

$$T = 1 + \frac{4\Delta\Phi^{(3)} a}{(a^2+1)(a^2+9)}, \tag{1}$$

where $\Delta\Phi^{(3)} = k n_2 I \left(\frac{1-\exp(-\alpha_0 L)}{\alpha_0}\right)$, k is the wavevector, n_2 is the third-order NL refractive index, α_0 is the linear absorption coefficient, L is the sample thickness, and $a = z/z_0$, where z is the sample position and z_0 the Rayleigh parameter. The value of $n_{NL} = +(4.2 \pm 0.3) \times 10^{-16}\ \mathrm{cm^2/W}$ was calculated using Eq. (1). We note that although we did not observe NLA in the low intensity ($<140\ \mathrm{GW/cm^2}$) regime, for intensities higher than $400\ \mathrm{GW/cm^2}$, NLA well above the noise floor (noise made the data unreliable between $140\ \mathrm{GW/cm^2}$ and $400\ \mathrm{GW/cm^2}$) was observed in the $ZrTe_2$ sample in ACN suspension, but it was also observed, with similar signal intensity, in ACN alone, and therefore it could not be unambiguously separated. Therefore,

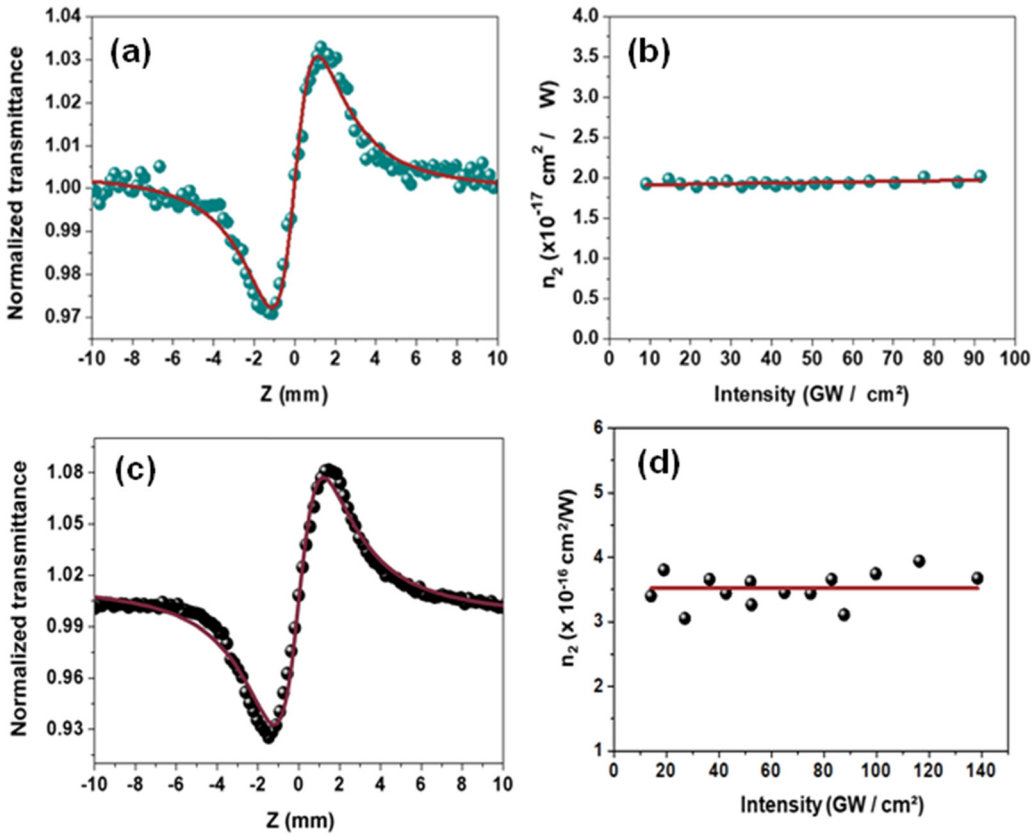

FIG. 2. Closed Aperture (CA) Z-scan curve for ACN at $I = 70\ GW/cm^2$ ($F = 44\ mJ/cm^2$); (b) intensity dependence of n_2; (c) closed aperture Z-scan curve for $ZrTe_2$ at $I = 42\ GW/cm^2$ ($F = 26.4\ mJ/cm^2$); and (d) intensity dependence of n_2 for $ZrTe_2$. The continuous lines are theoretical fits [see Eq. (1)].

our NLR data analysis was restricted to the range indicated above (maximum $140\ GW/cm^2$).

It can be instructive to compare the obtained nonlinear refractive index with that of other TMD suspensions under similar conditions. We have recently reported on the characterization of both MoS_2 (semiconductor) and NbS_2 (metal), respectively, obtaining nonlinear indices of $+(4.5 \pm 0.3) \times 10^{-16}\ cm^2/W$ and $+(3.0 \pm 0.2) \times 10^{-16}\ cm^2/W$ (the latter obtained beyond a critical intensity).[15] While the nonlinear refraction at 800 nm is similar for all three materials, important differences can be highlighted. While $ZrTe_2$ and MoS_2 do not exhibit measurable nonlinear absorption, this effect was observed for NbS_2. In addition, as MoS_2 is a semiconductor while $ZrTe_2$ is a semi-metal, the spectral dependence of their nonlinear refraction and absorption is certainly different, even though such a study is beyond the scope of the present letter.

To qualitatively explain the origin of the NLR in the 2D exfoliated $ZrTe_2$ monolayer suspension, its band structure was calculated using Density Functional Theory (DFT), as shown in Fig. 3. The calculation procedure followed the same as for NbS_2.[15] To summarize, we used *ab initio* methods based on Density Functional Theory (DFT), as implemented in SIESTA code.[26] We used exchange–correlation functional with nonlocal van der Waals (vdW) correction,[27] an energy mesh cutoff of 400 Ry, an energy shift of 0.03 eV, and a Monkhorst-Pack grid of $20 \times 20 \times 1$ for Brillouin zone k-point sampling.[28]

In the analysis of Fig. 3, the arrow length corresponds to the photon energy (1.55 eV) at the excitation wavelength (800 nm). They are placed in two possible positions in K-space, where the transition probability is higher compared to other positions. The one photon

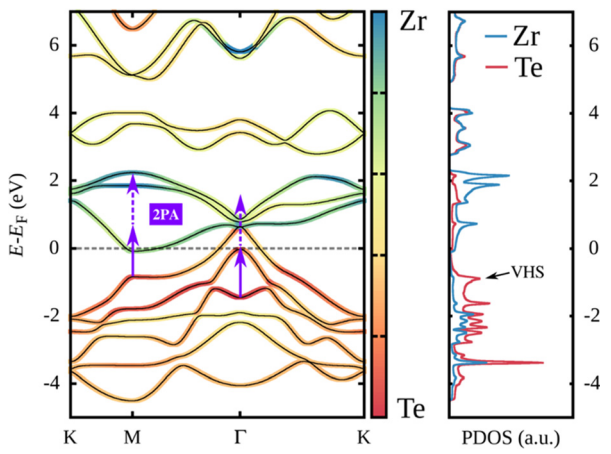

FIG. 3. Calculated band structure and projected density of states (PDOS) for $ZrTe_2$ using the DFT method. VHS indicates a van Hove singularity.

transitions corresponding to 1.55 eV are indicated by the heavy lines, whereas the dashed arrows indicate the additional 1.55 eV for a two-photon process. From the DFT calculations, it can be seen that there is no one photon transition from the valence to conduction band neither any two-photon transitions allowed by selection rule. This explains that, in this experimental regime, there is no (or negligible) absorption that can lead no nonlinear absorptive effects. Also, because the incident photon energy is below the gap corresponding to transitions to higher conduction bands, only virtual transitions occur, and the self-focusing nonlinear refraction measured is also explained by the band structure calculation. It should also be pointed out that off resonance transitions near point M of the band structure diagram are more likely, since they take advantage of a van Hove singularity, which indicates a higher oscillator strength. Clearly, changes in the bands' shape and in the distance between bands affect the optical nonlinearity of the TMD. Important differences can be observed in the band structure of bulk 1T $ZrTe_2$, as well as of monolayer $ZrTe_2$ in the 2H phase. Additionally, defects are known to add energy-localized states, which would also impact the obtained nonlinearity. Consequently, adjusting flake thickness, phase, and defect content can be useful tuning knobs for tailoring the optical nonlinearity.

In summary, we have reported on the third-order nonlinear optical studies of monolayer suspension of semi-metallic $ZrTe_2$ prepared by a modified redox exfoliated method. The experimental results, supported by theoretical DFT calculations, showed a positive NLR and no NLA at 800 nm, 100 fs, 1 kHz. This differs from recently reported work in a similar spectro-temporal and intensity regime with metallic NbS_2, whereby NLR and NLA were observed, and with a change in sign for NLR (from negative to positive) at a given intensity. Both values of n_2 in the range of 50–120 GW/cm^2 were in the same order of magnitude, $(3.0 \pm 0.1) \times 10^{-16}$ cm^2/W for NbS_2 and $(4.2 \pm 0.3) \times 10^{-16}$ cm^2/W for $ZrTe_2$. Further time-resolved experiments as well as a nonlinearity dispersion measurement will shed more light on the understanding of the fundamental of light–matter interaction in this nanomaterial.

AUTHORS' CONTRIBUTIONS

M.M. and M.L.d.S.N. contributed equally to this work.

The authors thank financial support from CNPq, FACEPE, and CAPES. A.S.L.G., C.J.S.d.M., P.G.V., and M.M. acknowledge support from AFOSR. A.M.J., A.J.R., and R.A.V. thank AFOSR and the Air Force Research Laboratory Materials and Manufacturing Directorate for financial support. C.J.S.d.M. acknowledges support from FAPESP (Thematic Projects Nos. 2015/11779-4 and 2018/25339-4), the Brazilian Nanocarbon Institute of Science and Technology (INCT/Nanocarbono), and CAPES−PRINT (Programa Institucional de Internacionalização; Grant No. 88887.310281/2018-00). L.S. acknowledges financial support of CNPq (Grant No. 408525/2018-5) and high-performance computing facilities of NACAD/COPPE, UFRJ. P.G.V. acknowledges CAPES for a Ph.D. fellowship. H.B.R. acknowledges FAPESP for post-doctoral fellowships (Grant Nos. 2018/04926-9 and 2017/20100-00).

DATA AVAILABILITY

The data that support the findings of this study are available from the corresponding author upon reasonable request.

REFERENCES

[1]E. Garmire, Opt. Express **21**, 30532 (2013).
[2]A. Prylepa, C. Reitböck, M. Cobet, A. Jesacher, X. Jin, R. Adelung, M. Schatzl-Linder, G. Luckeneder, K.-H. Stellnberger, T. Steck, J. Faderl, T. Stehrer, and D. Stifter, J. Phys. D **51**, 043001 (2018).
[3]N. M. Litchinitser, "Nonlinear optics in metamaterials," Adv. Phys.: X **3**, 1367628 (2018).
[4]A. S. L. Gomes, M. Maldonado, L. de S. Menezes, L. H. Acioli, C. B. de Araújo, J. Dysart, D. Doyle, P. Johns, J. Naciri, N. Charipar, and J. Fontana, Nanophotonics **9**(4), 725 (2020).
[5]J. W. You, S. R. Bongu, Q. Bao, and N. C. Panoiu, Nanophotonics **8**(1), 63 (2018).
[6]A. Autere, H. Jussila, Y. Dai, Y. Wang, H. Lipsanen, and Z. Sun, Adv. Mater. **30**(24), 1705963 (2018).
[7]Z. Wei, B. Li, C. Xia, Y. Cui, J. He, J.-B. Xia, and J. Li, Small Methods **2**, 1800094 (2018).
[8]D. Geng and H. Yang, Adv. Mater. **30**, 1800865 (2018).
[9]W. Choi, N. Choudhary, G. H. Han, J. Park, D. Akinwande, and Y. H. Lee, Mater. Today **20**(3), 116 (2017).
[10]S. A. Han, R. Bhatia, and S.-W. Kim, Nano Convergence **2**, 17 (2015).
[11]Z. Liu, B. Zhang, and Y. Chen, Chemistry **1**(1), 17 (2019).
[12]S. Bikorimana, P. Lama, A. Walser, R. Dorsinville, S. Anghel, A. Mitioglu, A. Micu, and L. Kulyuk, Opt. Express **24**(18), 20685 (2016).
[13]X. Zheng, Y. W. Zhang, R. Z. Chen, X. A. Cheng, Z. J. Xu, and T. Jiang, Opt. Express **23**, 15616 (2015).
[14]K. Wang, Y. Feng, C. Chang, J. Zhan, C. Wang, Q. Zhao, J. N. Coleman, L. Zhang, W. J. Blau, and J. Wang, Nanoscale **6**, 10530 (2014).
[15]M. Maldonado, M. L. S. Neto, P. G. Vianna, H. B. Ribeiro, V. O. Gordo, I. C. S. Carvalho, L. S. Menezes, C. B. de Araújo, C. J. S. de Matos, L. Seixas, A. M. Jawaid, R. Busch, A. J. Ritter, R. A. Vaia, and A. S. L. Gomes, J. Phys. Chem. C **124**, 15425 (2020).
[16]C. Yan, C. Gong, P. Wangyang, J. Chu, K. Hu, C. Li, X. Wang, X. Du, T. Zhai, Y. Li, and J. Xiong, Adv. Funct. Mater. **28**, 1803305 (2018).
[17]A. Jawaid, J. Che, L. F. Drummy, J. E. Bultman, A. Waite, M.-S. Hsiao, and R. A. Vaia, ACS Nano **11**, 635 (2017).
[18]A. Jawaid, A. J. Ritter, and R. A. Vaia, Chem. Mater. **32**(15), 6550 (2020).
[19]M. Sheik-Bahae, A. A. Said, T.-H. Wei, D. J. Hagan, and E. W. Van Stryland, IEEE J. Quantum Electron. **26**, 760 (1990).
[20]C. B. de Araújo, A. S. L. Gomes, and G. Boudebs, Rep. Prog. Phys. **79**, 036401 (2016).
[21]P. Tsipas, D. Tsoutsou, S. Fragkos, R. Sant, C. Alvarez, H. Okuno, G. Renaud, R. Alcotte, T. Baron, and A. Dimoulas, ACS Nano **12**(2), 1696–1703 (2018).
[22]I. Kar, J. Chatterjee, L. Harnagea, Y. Kushnirenko, A. V. Fedorov, D. Shrivastava, B. Büchner, P. Mahadevan, and S. Thirupathaiah, Phys. Rev. B **101**, 165122 (2020).
[23]Z. Muhammad, B. Zhang, H. Lv, H. Shan, Z. Rehman, S. Chen, Z. Sun, X. Wu, A. Zhao, and L. Song, ACS Nano **14**, 835 (2020).
[24]P. I. R. Pincheira, M. L. S. Neto, M. Maldonado, C. B. de Araújo, A. M. Jawaid, R. Busch, A. J. Ritter, R. A. Vaia, and A. S. L. Gomes, Nanoscale **12**, 15706 (2020).
[25]K. Iliopoulos, D. Potamianos, E. Kakkava, P. Aloukos, I. Orfanos, and S. Couris, Opt. Express **23**, 24171 (2015).
[26]J. M. Soler, E. Artacho, J. D. Gale, A. Garcia, J. Junquera, P. Ordejon, and D. Sanchez-Portal, J. Phys. **14**, 2745 (2002).
[27]O. A. Vydrov and T. Van Voorhis, J. Chem. Phys. **133**, 244103 (2010).
[28]H. J. Monkhorstand and J. D. Pack, Phys. Rev. B **13**, 5188 (1976).